NUMERICAL INVESTIGATION OF TURBULENT FLOW THROUGH RADIAL DIFFUSER

Lincoln Batista
Mechanical Engineering Undergraduate Program

William de Araújo Jacques
Mechanical Engineering Graduate Program – PPGEM
william.jacques@pucpr.br

Viviana Cocco Mariani
Mechanical Engineering Graduate Program – PPGEM
Pontifical Catholic University of Parana – PUCPR
80215-901 – Curitiba, PR, Brazil
viviana.mariani@pucpr.br

Abstract. *Experimentally validated numerical analysis of the incompressible turbulent isothermal flow between concentric parallel disks has been performed. Most reciprocating compressors used in domestic refrigerators employ automatic valves that open and close depending on the pressure difference across them. In this valves the flow is supplied axially by a feeding orifice placed in one of the disks and becomes radial after being deflected by the frontal disk. The bi-dimensional governing equations with low Reynols number k-ε model being employed for the turbulence modeling are solved using the finite volume methodology. Coupling between pressure and velocity was handled through the SIMPLE algorithm and Power Law Differencing and QUICK scheme were adopted to approximate the variables at the control volume faces. The numerical model was validated through comparison of experimental radial pressure profiles of the literature. The characteristics of the flow with respect to the gap between the disks and differents Reynolds numbers are analyzed through radial presssure profiles and property flow fields such as effective flow and force areas and force which are important efficiency parameters for the modelling and design of reciprocating hermetic compressors. It is found that the pressure distribution on the disk surface is significantly affected by gap between disks with the diameter tested. The results show that the k-ε model is efficient predicting adequately this class of flow.*

Keywords*: turbulent flow, radial diffuser, k-ε model, finite volume methodology*

1. INTRODUCTION

Reed valves are essential components in a number of compressors, particularly the hermetic ones employed in refrigeration. These valves are called automatic because they open and close depending on the pressure difference between the cylinder and the suction/discharge chamber, established by the piston motion. Once the valves are open, the pressure flow field is responsible for the resultant force acting on the reed. In designing the valve system for reciprocating compressors four main features related to the valve performance are sought: fast response, high mass flow rate, low pressure drop when opened, and good backflow blockage when closed (Rovaris and Deschamps, 2006). To satisfy the performance requirements necessary for a competitive compressor, a detailed understanding of the fluid flow through the valve as well as the dynamics of the valve is necessary.

Valve performance is an intricate problem where fluid mechanics and solid dynamics play a definite role. The basic features related to the flow across the valve and the reed dynamics can be explained in Fig. 1, where a simplified discharge valve is represented by a circular disk. In this valve the fluid flows axially through a feeding orifice with diameter *d*, and then is deflected along the radial direction by the frontal disk, represented in the figure by the valve reed with diameter *D*. In the present investigation the flow is assumed turbulent and axially symmetric. The pressure difference between the orifice entrance and the discharge chamber together with the valve lift govern the fluid flow throughout the valve. On the other hand, the flow dictates the pressure distribution on the reed and, consequently, the resultant force that will govern the valve dynamics and its displacement from the seat.

In the context of valves, a number of important studies can be cited, such as: Deschamps *et al.* (1996), Lopes and Prata (1997), Ezzat Khalifa and Liu (1998), Salinas-Casanova *et a*l. (1999), Chung *et al.* (2000), Matos *et al*. (2000). In Matos *et al*. (2002) a three-dimensional model was used to simulate the complete compression cycle, including the turbulent flow through the discharge valve. Turbulence contribution to the flow transport was accounted for with the RNG *k-*ε model. The methodology was found to return a precise description of physical mechanisms that influence the compressor efficiency, such as heat transfer at the cylinder wall and transient effects on the valve dynamics, however the computational processing time was excessive for compressor design purposes. Rovaris and Deschamps (2006) reduced the computational time of Matos *et al.* (2002) with the same level of accuracy. The solution procedure combined integral and differential formulations. The compressible turbulent flow through the discharge valve was

predicted via large-eddy simulation (LES), with the Smagorinsky model for the sub-grid scale motions. Results were seen to capture several important phenomena that occur in the discharge process, such as pressure over shooting in the cylinder and backflow through the discharge valve.

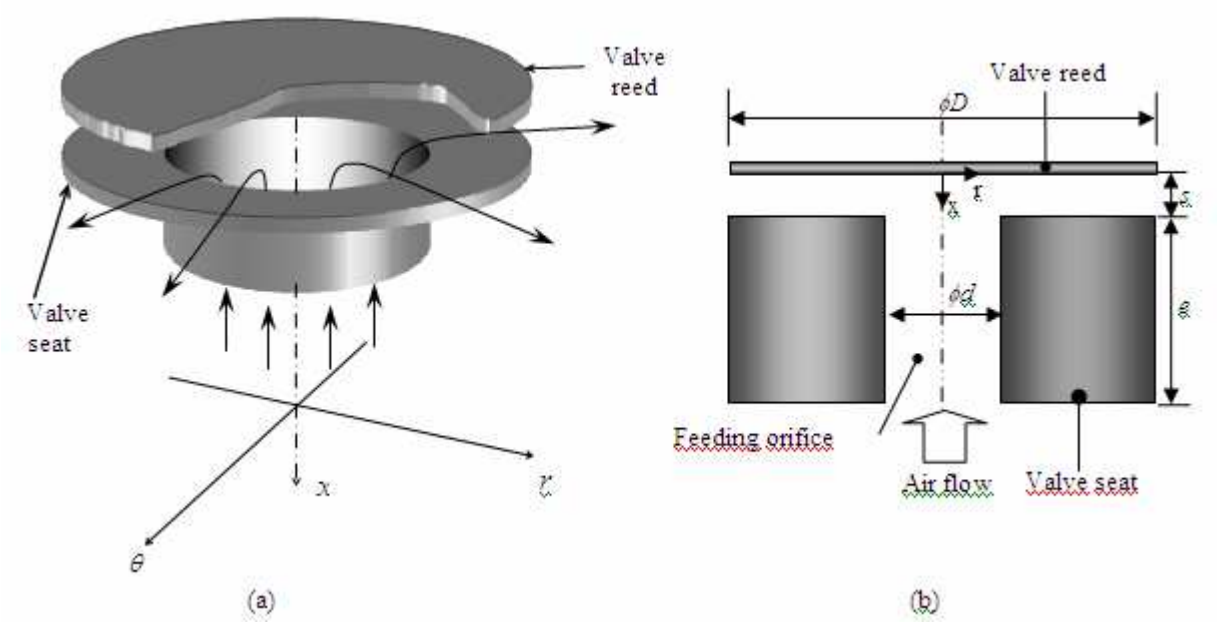

Figure 1 – Geometry of radial diffuser.

The main objective of this work is to solve bi-dimensional turbulent governing equations with low Reynols number k-ε model, using the finite volume methodology. Power Law Differencing and QUICK schemes are adopted to approximate the variables at the control volume faces. The numerical model is validated through comparison of experimental radial pressure profiles along the valve reed obtained in the literature. The characteristics of the flow with respect to the gap between the disks and differents Reynolds numbers are analyzed through radial presssure profiles and property flow fields such as effective flow and force areas and force which are important efficiency parameters.

2. TURBULENCE MODELING

Reynolds decomposed the Navier-Stokes equations in two parties, one related to the average value of the velocity vector and another related to its fluctuation, and applied the time average operator to study turbulent flows. The resulting set of equations is known as Reynolds Average Navier-Stokes (RANS) equations and gives information about the mean flow. Although this approach is not able to describe the multitude of length scales involved in turbulence, it has been largely used because in many engineering applications the information about the mean flow is satisfactory. For an isothermal and incompressible flow under the effect of no body force the equations of motion, writen in Cartesian tensor notation, can be expressed by,

$$\frac{\partial U_i}{\partial x_i} = 0\,, \tag{1}$$

$$\frac{\partial (U_i U_j)}{\partial x_j} = -\frac{1}{\rho}\frac{\partial P}{\partial x_i} + \frac{\partial}{\partial x_j}\left(\nu \frac{\partial U_i}{\partial x_j} - \overline{u_i u_j}\right), \tag{2}$$

where U_i and U_j are components of the average velocity vector [m/s], ρ is the fluid density [kg/m^3], $\nu = \mu/\rho$ is the kinematic viscosity, μ is the dynamic viscosity of the fluid [Pa.s], P is the mean average pressure [Pa]. The extra-term that appears in Eq. (2) comparing to the original Navier-Stokes equations, $\overline{u_i u_j}$, is the product of fluctuation velocities [m^2/s^2] denoted by Reynolds stresses and is never negligible in any turbulent flow. It represents the increase in the diffusion of the mean flow due to the turbulence. Equations (1) and (2) can only be solved if the Reynolds stress tensor are known, a problem referred to as the "closure problem" since the number of unknowns is greater than the number of equations.

The main goal of the turbulence studies based on the RANS equations is to determine the Reynolds stresses. According to Kolmogorov (1942) they can be evaluated by the following expression:

$$-\overline{u_i u_j} = \nu_t \left(\frac{\partial U_i}{\partial x_j} + \frac{\partial U_j}{\partial x_i} \right) - \frac{2}{3} \delta_{ij} k \,, \tag{3}$$

where δ_{ij} is the Kronecker delta and the kinetic energy of the turbulent motion, k, is defined as $k = \overline{u_i u_i}/2$ [m^2/s^2]. Substitution of Eq. (3) into Eq. (2) results in the average Navier-Stokes equations with the Reynolds stresses modeled by viscosity concecpt,

$$\frac{\partial (U_i U_j)}{\partial x_j} = -\frac{1}{\rho} \frac{\partial}{\partial x_i} \left(P + \frac{2}{3} \rho k \right) + \frac{\partial}{\partial x_j} \left[\nu_{eff} \left(\frac{\partial U_i}{\partial x_j} + \frac{\partial U_j}{\partial x_i} \right) \right] \tag{4}$$

where $\nu_{eff} = \nu + \nu_t$. The turbulent viscosity can be expressed as the product of a velocity scale, u [m/s], and a length scale, L_μ [m], $\mu_t = \rho u L_\mu$. Considering the velocity scale being calculated by $u = \sqrt{k}$, Kolmogorov (1942) and Prandtl (1945) independently proposed the following relation for the turbulent viscosity,

$$\nu_t = c_\mu k^{1/2} L_\mu \,, \tag{5}$$

where $c_\mu = 0.09$ is an empiric constant.

To close the set of equations described above, the most popular turbulence models define two other transport equations: one for the turbulent kinectic energy, k, and another for a variable that relates k to L_μ. These models are called two equations models, and one of them have been employed in this work the low Reynols number k-ε model of Launder and Sharma (1974).

Due to its robustness, economy and acceptable results for a considerable amount of flows, the k-ε model has been used frequently for numerical predictions of industrial flows. However, it has deficiencies in some situations involving streamline curvatures, acceleration and separation. Although the present flow has the characteristics cited previously, decided use in this work the k-ε model.

In this model the second variable for the complementary transport equations is the rate of the viscous dissipation, ε [m^2/s^3], which is related to k by:

$$\varepsilon = k^{3/2} / L \,. \tag{6}$$

The first low Reynols number k-ε model was proposed Jones and Launder (1972). The model adopt the $\tilde{\varepsilon}$ variable

$$\tilde{\varepsilon} = \varepsilon - 2\nu \left(\frac{\partial \sqrt{k}}{\partial x_i} \right)^2 \,. \tag{7}$$

in the place of ε, for the simple reason that the boundary condition in walls for $\tilde{\varepsilon}$ is easier. The amortecimento factor

$$f_\mu = e^{\left[-3.4/(1+R_t/20)^2 \right]} \,. \tag{8}$$

is introduced in the turbulent viscosity,

$$\nu_t = f_\mu c_\mu \frac{k^2}{\tilde{\varepsilon}} \,. \tag{9}$$

where R_t is turbulent Reynolds.

The Jones and Launder (1972) model was optimized by Launder and Sharma (1974) and the equations for k and $\tilde{\varepsilon}$ are, respectively, given by,

$$\frac{\partial(U_j k)}{\partial x_j} = \frac{\partial}{\partial x_j}\left[\left(\nu + \frac{\nu_t}{\sigma_k}\right)\frac{\partial k}{\partial x_j}\right] + \nu_t\left[\frac{\partial U_i}{\partial x_j} + \frac{\partial U_j}{\partial x_i}\right]\left[\frac{\partial U_i}{\partial x_j}\right] - \tilde{\varepsilon} - 2\nu\left(\frac{\partial \sqrt{k}}{\partial x_j}\right)^2 \tag{10}$$

$$\frac{\partial(U_j \tilde{\varepsilon})}{\partial x_j} = \frac{\partial}{\partial x_j}\left[\left(\nu + \frac{\nu_t}{\sigma_\varepsilon}\right)\frac{\partial \tilde{\varepsilon}}{\partial x_j}\right] + f_1 c_1 \nu_t \frac{\tilde{\varepsilon}}{k}\left[\frac{\partial U_i}{\partial x_j} + \frac{\partial U_j}{\partial x_i}\right]\left[\frac{\partial U_i}{\partial x_j}\right] - f_2 c_2 \frac{\tilde{\varepsilon}^2}{k} + 2\nu\nu_t\left(\frac{\partial^2 U_i}{\partial x_k \partial x_l}\right)^2 \tag{11}$$

where $c_1 = 1.42$; $c_2 = 1.92$; $\sigma_k = 1$ e $\sigma_\varepsilon = 1.22$ are empirical constants, $f_1 = 1$, $f_2 = 1 - 0.3e^{-R_t^2}$. The functions f_1, f_2 and f_μ are introduced for to correct the empirical constants in regions where viscous efects are important.

In order to solve Eqs. (4), (10) and (11) boundary conditions are required at inlet, walls, axis of symmetry and outlet, such conditions were based in work of Deschamps (2000). The inlet boundary conditions for the axial and radial velocity components were specified as $U = U_{in}$ and $V = 0$, respectively, with U_{in} being the average velocity in the orifice. Although no information is available for the turbulence kinetic energy, numerical tests indicated that when the level of the turbulence intensity I, based on U_{in}, is increased from 3% to 6% no significant change is observed in the predicted flow. Therefore, an intensity of 3% was used in the calculation of all results shown in this work. Finally, the distribution of the dissipation rate was estimated based on the assumption of equilibrium boundary, that is

$$\tilde{\varepsilon}_{in} = \frac{c_\mu^{3/4} k^{3/2}}{L_m} \tag{12}$$

with the mixing length, L_m, being calculated using an empirical coefficient for turbulent pipe flow, that is, $L_m = 0.07d/2$,

At the solid boundaries the condition of no-slip and impermeable wall boundary condition were imposed for the velocity components, that is, $U = V = 0$, with calculations being extended up to the walls across the viscous sublayer. The turbulente quantities are nulls at the walls. In the plane of symmetry, the normal velocity and the normal gradients of all other quantities were set to zero. At the outlet boundary a condition of parabolic flow can be assumed.

As a common practice, Eqs. (4), (10) and (11) can be express by one unique equation for the generic variable, ϕ, such as,

$$\frac{\partial(U_j \phi)}{\partial x_j} = \frac{\partial}{\partial x_j}\left(\Gamma^\phi \frac{\partial \phi}{\partial x_j}\right) + S^\phi, \tag{13}$$

where ϕ is equal to U and V for Eq. (4), k for Eq. (10), $\tilde{\varepsilon}$ for Eq. (11), and equal to unity for continuity equation, Γ^ϕ and S^ϕ are, respectively, the diffusion coefficient and term source. The Eq. (13) will be discretized in the next section.

2.2 Numerical Methodology

A finite volume discretization scheme was used to solve the governing differential equations. According to this practice the solution is divided into small non-overlapping control volumes and the continuity, momentum and turbulence quantities differential equations are integrated over each control volume (Patankar, 1980; Versteeg e Malalasekera, 1995). The resulting system of algebraic equations is solved using a combination of the Thomas algorithm method (Patankar, 1980). Prior to solving the algebraic system of equations the discretized form of the continuity equation was transformed into an equation for pressure using the SIMPLE methodology. Interpolations of unknown quantities at the control volume faces were obtained using the QUICK scheme (Hayase *et al*., 1992) and Power Law Differencing scheme (PLDS) (Patankar, 1980).

Here will be presented only discretized equation using PLDS scheme for control volume central, P, as ilustrated in Fig. 2.

$$A_p \phi_P = A_e \phi_E + A_w \phi_W + A_n \phi_N + A_s \phi_S + S_P \tag{14}$$

where,

$$
\begin{aligned}
A_e &= D_e A\left|Pe_e\right| + \max(-F_e,0)\\
A_w &= D_w A\left|Pe_w\right| + \max(F_w,0)\\
A_n &= D_n A\left|Pe_n\right| + \max(-F_n,0)\\
A_s &= D_s A\left|Pe_s\right| + \max(F_s,0)\\
A_P &= A_e + A_w + A_n + A_s
\end{aligned}
\tag{15}
$$

In Eq. (15) the function max(a, b) obtain the value maximum between a and b, $A|Pe| = max(0,(1\text{-}0{,}1|Pe|)^5)$, $D_e = \frac{r_P \Delta r \Gamma_e^{\phi}}{\Delta x_e}$, $D_w = \frac{r_P \Delta r \Gamma_w^{\phi}}{\Delta x_w}$, $D_n = \frac{r_n \Delta x \Gamma_n^{\phi}}{\Delta r_n}$, $D_s = \frac{r_s \Delta x \Gamma_s^{\phi}}{\Delta r_s}$, $F_e = \rho_e U_e r_P \Delta r$, $F_w = \rho_w U_w r_P \Delta r$, $F_n = \rho_n V_n r_n \Delta x$, $F_s = \rho_s V_s r_s \Delta x$. The terms S_P for governing equations are described in Tab. 1.

Table 1 - Terms source for equation generic ϕ.

ϕ	S_P
1	0
U	$-\left[\left(p_e + 2/3\rho_e k_e\right) - \left(p_w + 2/3\rho_w k_w\right)\right]\frac{r_P}{\rho_P}\Delta r - \left[\frac{\nu_t^e}{\Delta x_e \Delta x} + \frac{\nu_t^w}{\Delta x_w \Delta x}\right]\Delta V U_P + \frac{\nu_t^e \Delta V}{\Delta x_e \Delta x}U_E + \frac{\nu_t^w \Delta V}{\Delta x_w \Delta x}U_W + \frac{r_n \nu_t^n \Delta V}{\Delta x r \Delta r}(V_{ne} - V_{nw}) - \frac{r_s \nu_t^s \Delta V}{\Delta x r \Delta r}(V_{se} - V_{sw})$
V	$-\left[\left(p_n + 2/3\rho_n k_n\right) - \left(p_s + 2/3\rho_s k_s\right)\right]\frac{r_P}{\rho_P}\Delta x - \left[\frac{\nu_P}{r_P^2} + 2\frac{\nu_t^P}{r_P^2} + \frac{r_n \nu_t^n}{r_P \Delta r \Delta r_n} + \frac{r_s \nu_t^s}{r_P \Delta r \Delta r_s}\right]\Delta V V_P + \frac{r_n \nu_t^n \Delta V}{r_P \Delta r \Delta r_n}V_N + \frac{r_s \nu_t^s \Delta V}{r_P \Delta r_s \Delta r}V_S + \frac{\nu_t^e \Delta V}{\Delta x \Delta r}(U_{ne} - U_{se}) - \frac{\nu_t^w \Delta V}{\Delta x \Delta r}(U_{nw} - U_{sw})$
k	$\nu_t^P\left[2\left(\frac{U_e - U_w}{\Delta x}\right)^2 + 2\left(\frac{V_n - V_s}{\Delta r}\right)^2 + 2\left(\frac{V_P}{r_P}\right)^2 + 2\left(\frac{U_n - U_s}{\Delta r} - \frac{V_e - V_w}{\Delta x}\right)^2\right]\Delta V + -2\nu_t\left[\left(\frac{\sqrt{k}_e - \sqrt{k}_w}{\Delta x}\right)^2 + \left(\frac{\sqrt{k}_n - \sqrt{k}_s}{\Delta y}\right)^2\right]\Delta V - \tilde{\varepsilon}_P \Delta V$
$\tilde{\varepsilon}$	$c_1 f_1 \frac{\tilde{\varepsilon}_P}{k_P}\nu_t^P\left[2\left(\frac{U_e - U_w}{\Delta x}\right)^2 + 2\left(\frac{V_n - V_s}{\Delta r}\right)^2 + 2\left(\frac{V_P}{r_P}\right)^2 + 2\left(\frac{U_n - U_s}{\Delta r} - \frac{V_e - V_w}{\Delta x}\right)^2\right]\Delta V - c_2 f_2 \frac{\tilde{\varepsilon}_P^2}{k_P}\Delta V + 2\nu\nu_t\left[\left(\frac{\left(\frac{\partial U}{\partial y}\right)_n - \left(\frac{\partial U}{\partial y}\right)_s}{\Delta y}\right)^2 + \left(\frac{\left(\frac{\partial V}{\partial x}\right)_e - \left(\frac{\partial V}{\partial x}\right)_w}{\Delta x}\right)^2\right]\Delta V$

Due to the strong non-linearity of the equations, under relaxation coefficients were required. For the velocity components these coefficients were 0.1, for pressure 0.1 and for the turbulence quantities was used 0.75. Convergence was stopped when the maximum residual of the algebraic equations was less than 10^{-4}. All results to be presented were obtained with a mesh consisted of 70 × 80 grid points (circunferencial × radial). All points were hand placed with higher concentration in the regions of steeper gradients. The final mesh adopted in performing the computations was chosen after several grid independence tests that were carried in Salinas-Casanova *et al.* (1999).

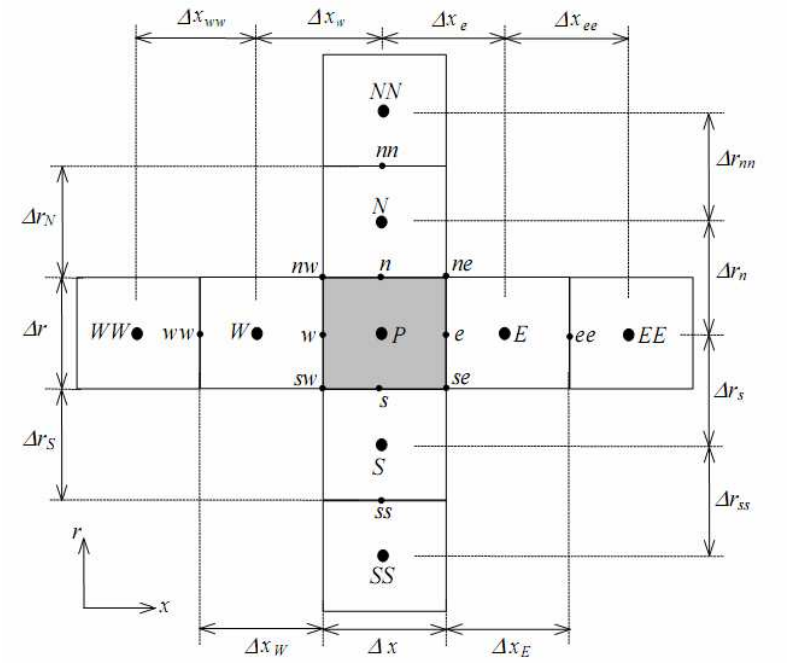

Figure 2 – Control volume *P*.

3. RESULTS AND DISCUSSIONS

The numerical model was first validated through comparisons of dimensionless pressure on the front disk given by

$$p^* = 2p/(\rho U_{in}^2) \tag{16}$$

obtained with k-ε model and comparing with experimental datas presented in Salinas-Casanova *et al.* (1999) and Deschamps *et al.* (2000). The flow through the radial diffuser presented in Fig. 1 was investigated for three displacements, *s/d* (= 0.03, 0.05 and 0.07) and three Reynolds number, *Re* (= 18,800; 20,100 and 25,000) and one diameter ratio, *D/d* = 3. In all cases, the feeding orifice length was *e/d* = 1.0423. The cases studied in the present work are solved by k-ε model and such cases are presented in Fig. 3.

The good agreement between experimental and numerical values seen in Fig. 4 provided confidence in the turbulence model used, mainly for QUICK scheme that was used in the remainder of the work. In Figs. 4-6 the pressure profile exhibts a plateau on the central part of the curve (r/d < 0.5), as previously verified for the laminar flow by Ferreira and Driessen (1986) and for the turbulent flow by Salinas-Casanova *et al.* (1999), Deschamps *et al.* (2000) and Matos *et al.* (2002). Also similar to the laminar flow is the sharp pressure drop at the radial position r/d = 0.5, which is due to the change in the flow direction. For the r/d > 0.5 the pressure level never recovers a positive value, a situation which is verified also in the laminar flow for combinations of both large displacement and high Reynolds number.

Considering three displacements (s/d = 0.03, 0.05 and 0.07) and one Reynolds number is shown the Fig. 5, where can be see that the pressure distribution on the disk surface is dependent on the gap between disks. The results presented in Fig. 6 show no significant difference between the pressure distributions on the valve surface for the Reynolds numbers analysed, main for Reynols number 18,800 and 20,100.

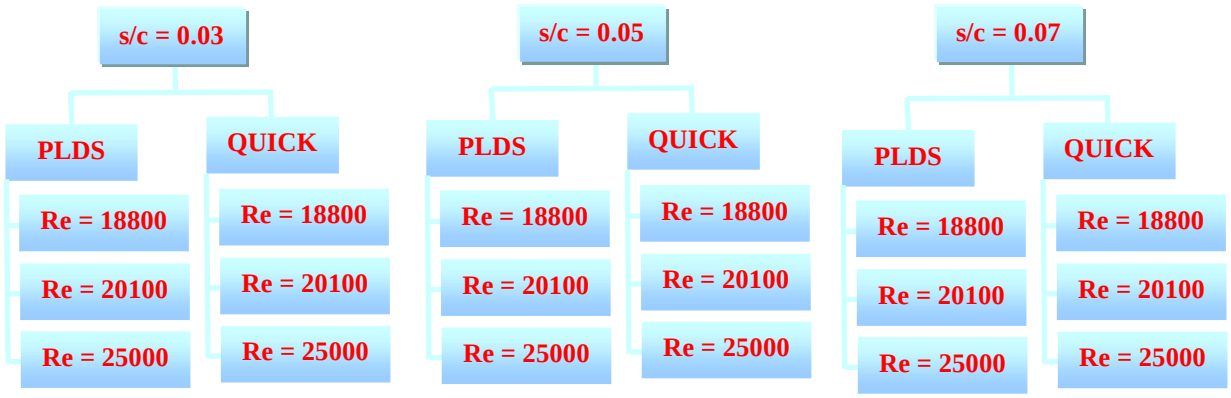

Figure 3 - Cases studied in the present work.

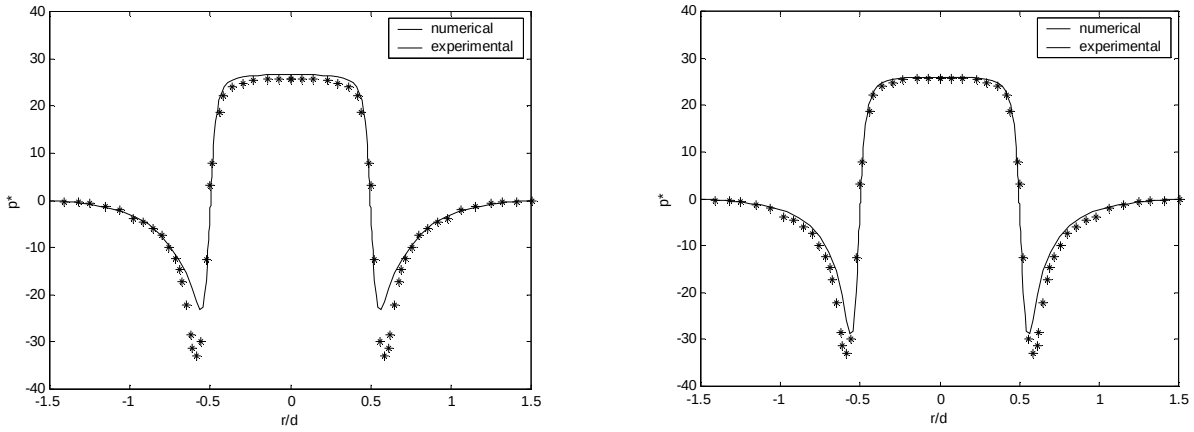

PLDS **QUICK**

Figure 4 – Numerical and experimental results for pressure distribution along valve reed for *s/d* = 0.05 and *Re* = 25,000 with PLDS and QUICK.

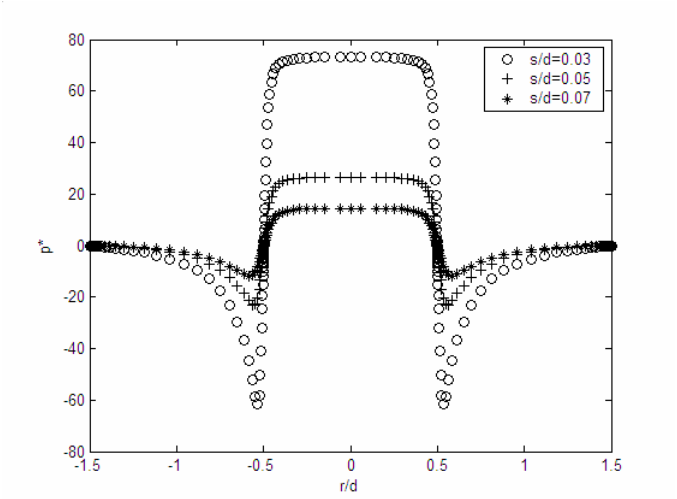

Figure 5 – Sensitivity of results for pressure distribution along valve reed to gap between disks: *s/d* = 0.03, 0.05 and 0.07, for *Re* = 20,100.

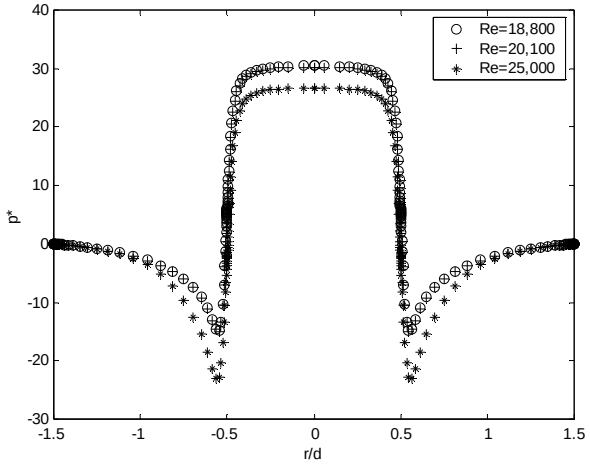

Figure 6 – Sensivity of results for pressure distribution along valve reed to Reynolds numbers: *Re* = 18,800; 20,100 and 25,000, for *s/d* = 0.05.

3.1 Parameter efficiency

As explored before, two parameters are very important in valve modeling and design: the effective flow and force areas. Those two parameters are generally used in numerical simulation of reciprocating hermetic compressors and can also be employed to evaluate the efficiency of the valves.

The effective flow area, A_{ee}, is directly related to the pressure drop through valve. For a given pressure drop A_{ee} can yield the mass flux through the valve. Thus, the higher the $A_{ee,}$ the better is the performance of the valve with respect to the flow through it (Ussyk, 1984). The effective flow area is defined as

$$A_{ee} = \frac{\dot{m}}{p_u \sqrt{\frac{2\mathrm{k}}{(\mathrm{k}-1)\mathrm{R}T_u}} \sqrt{r_p^{\,2/\mathrm{k}} - r_p^{\,(\mathrm{k}+1)/\mathrm{k}}}} \tag{17}$$

where $\dot{m}$ is the mass flow rate through the valve, $r_p = p_{atm}/p_u$, p_{atm} is the atmospheric pressure, p_u is the pressure upstream the valve, $k = c_p/c_v$, R is the gas constant, and T_u is the temperature upstream the valve. The dimensionless effective flow area is calculated by $A_{eea} = 4A_{ee}/\pi d^2$.

Results for dimensionles A_{eea} are shown in Tab. 3 for *s/d* = 0.03, 0.05 and 0.07. As seen from the Tab. 3 in general, the dimensionless effective flow area increases with the increasing value of the Reynolds numbers and of the gap between disks.

The effective flow area is important in predicting the mass flow rate through the valve during suction and discharge. However, to calculate the valve movement it is necessary to know the force acting on the reed during each instant of time. This force is a result of the difference in pressure acting on both sides of the valve and depends on the flow and on the opening of the reed (Schwerzler and Hamilton, 1972). Usually the force on the valve is calculated through the effective force area, defined as,

$$A_{ef} = F/\Delta p_v \tag{18}$$

where Δp_v is the pressure difference through the valve. The Tab. 3 shows the variation of the dimensionless effective force area ($A_{efa} = 4A_{ef}/\pi d^2$) for *s/d* = 0.03, 0.05 and 0.07 as a function of Reynolds numbers varying from 20,100 to 25,000. For the gap between seat and reed investigated in this work, the dimensionless effective force area exhibits a monotonic behavior similar to that observed for the effective flow area, that is, when Reynolds number increases the effective force area decreases. When crease the gap between disks decrease dimensionless effective force area.

Table 2 – Dimensionless effective flow area.

Re	s/d = 0.03	s/d = 0.05	s/d = 0.07
20100	0.1631	0.3711	0.3729
25000	0.1667	0.4077	0.4344

Table 3 – Dimensionless effective force area.

Re	s/d = 0.03	s/d = 0.05	s/d = 0.07
20100	-0.0618	-1,4810	-1.4959
25000	-0.1341	-1,8644	-1.7243

3.2 Force

The integration of the pressure distribution along the valve disc yielded the total force on the valve. The force is obtained by expression

$$F = 2\pi \int_0^{D/2} prdr \, . \tag{19}$$

Results for the dimensionless force

$$F^* = \frac{2F}{\rho U_{in}^2 d^2} \, , \tag{20}$$

are given in Tab. 4 for each gap between disks studied in this work. For each gap three Reynolds number are considered, *Re* = 18,800; 20,100 and 25,000. Because the dimensionless force has an average velocity raised to the square in the denominator, the *F** values for *Re* = 20,100 are in general higher than those for *Re* = 25,000.

Table 4 – Dimensionless force.

Re	s/d = 0.03	s/d = 0.05	s/d = 0.07
20100	-1.8254	-8.4463	-8.4480
25000	-3.7976	-8.8076	-7.1767

4. CONCLUSIONS

The present work has presented a numerical investigation of the incompressible 2D turbulent and isothermal flow in a radial diffuser. The flow was investigated for different parameters such as Reynolds number and gap between the disks. The k-ε turbulence model used to predict the flow was found to reproduce well the experimental results. New results must be obtained for a complet assessment of the turbulence model. The present work explored also the impact which small changes in the gap between disks have on the pressure, force, effective flow and force areas. The current analysis concluded that small modifications in the gap cause change in force, effective flow and force areas.

5. ACKNOWLEDGMENTS

The support of Associação Paranaense de Cultura, APC, in providing scholarships for the first and second authors is greatly appreciated. This work is part of a project under Grant 3-1-9130/2007 between Pontifical Catholic University of Paraná and Fundação Araucária.

6. REFERENCES

Chung, M.K., Baek, S.J., Lee, I.S., Rew, H.S., Bae, Y.J., Moon, Y.H. and Yun, T.W. 2000, "A Study on the Flow in a Discharge System of the Reciprocating Compressor using Computational Simulation and PIV", Proc. Compressor Engineering Conference at Purdue, West Lafayette, Indiana, USA, pp. 377-382.

Deschamps, C.J., Ferreira, R.T.S. and Prata A.T., 1996, "Turbulent Flow through Valves of Reciprocating Compressors", Proc. Compressor Engineering Conference at Purdue, West Lafayette, Indiana, USA, pp. 377-382.

Deschamps, C. J., Prata, A. T. and Ferreira, R. T. S., 2000, "Modeling of turbulent flow through radial diffuser", Journal of the Brazilian Society of Mechanical Sciences, Vol. XXII, no. 1, pp. 31-41.

Ezzat Khalifa, H. and Liu, X., 1998, "Analysis of Stiction Effect on the Dynamics of Compressor Suction Valve", Proc. Compressor Engineering Conference at Purdue, West Lafayette, Indiana, USA, pp. 87-92.

Ferreira, R. T. S. and Driessen, J. L., 1986, "Analysis of the Influence of Valve Geometric Parameters on the Effective Flow and Force Areas", Proc. 9th Purdue Int. Compressors Technology Conference, West Lafayette, USA, pp. 632-646.

Jones, W. P. and Launder, B. E., 1972, "The Calculation of Low-Reynolds-Number Phenomena with a Two-Equation Model of Turbulence", Int. Journal Heat and Mass Transfer, 16, pp. 1119-1130.

Kolmogorov, A.N., 1942, “Equations of turbulent motion of an incompressible fluid”. Izvestia Acad. Sci., USSR; Phys. 6 (1–2), pp. 56–58.
Launder, B. E.; Sharma, B. I., 1974, “Application of the Energy Dissipation Model of Turbulence to the Calculation of Flow Near Spinning Disc”. Letters in Heat and Mass Transfer, vol. 1 No. 2, pp. 131-138.
Lopes, M.N. and Prata, A.T., 1997, “Dynamic Behavior of Plate Type Valves in Periodic Flows” (in Portuguese), Proc. XIV Brazilian Congress of Mechanical Engineering, Bauru, Brazil.
Matos, F. F. S., 2002, “Análise Numérica do Comportamento Dinâmico de Válvulas Tipo Palheta em Compressores Alternativos”, Tese de Doutorado, Curso de Engenharia Mecânica, Universidade Federal de Santa Catarina, Brasil.
Matos, F.F.S., Prata, A.T. and Deschamps, C.J., 2000, “A Numerical Methodology for the Analysis of Valve Dynamics”, Proc. Compressor Engineering Conference at Purdue, West Lafayette, Indiana, USA, pp. 383-390.
Matos, F.F.S., Prata, A.T. and Deschamps, C.J., 2002, "Numerical Simulation of the Dynamics of Reed Type Valves", Proc. 2002 International Compressor Engineering Conference at Purdue (CD-ROM), West Lafayette, USA, 8 p.
Patankar, S. V., 1980, “Numerical Heat Transfer and Fluid Flow”, McGraw-Hill.
Possamai, F. C., Ferreira, R. T. S. and Prata, A. T., 2001, “Pressure distribution in laminar radial flow through inclined disks”, International Journal of Heat and Fluid Flow, 22, pp. 440-449.
Prandtl, L., 1945, “”Über ein neues formelsystem für die ausgebildete turbulenz”, Nachr. Akad. Wiss., Math-Phys. Kl, 6.
Salinas-Casanova., D. A., 2001, “Análise Numérica do Escoamento Turbulento em Válvulas Automáticas de Compressores”, Tese de Doutorado, Curso de Engenharia Mecânica, Universidade Federal de Santa Catarina, Brasil.
Salinas-Casanova, D. A., Deschamps, C.J. and Prata, A.T., 1999, “Turbulent Flow through a Valve with Inclined Reeds”, Proc. International Conference on Compressors and Their Systems, Londres, pp. 443-452.
Schwerzler, D. D. and Hamilton, J. F., 1972, “An Analitical for Determining Effective Flow and Force Areas for Refrigeration Compressor Valving Systems”, International Compressor Engineering Conference at Purdue, West Lafayette, Indiana, Vol. I, pp. 30-36.
Versteeg, H. K., Malalasekera, W., 1995, “An Introduction to Computational Fluid Dynamics”, Longman Scientific & Technical, New York.

7. RESPONSIBILITY NOTICE

The authors are the only responsible for the printed material included in this paper.